

Incoherent time evolution on a grid of Landau-Zener anticrossings

David A. Harmin and Phillip N. Price*

Department of Physics and Astronomy, University of Kentucky, Lexington, Kentucky 40506-0055

(Received 6 July 1993)

The mixing of Rydberg manifolds, induced by a ramped electric field $F(t) = \dot{F}t$, is modeled by interactions among two intersecting groups of parallel energy levels. The levels form a grid, each node of which is treated as an isolated two-level Landau-Zener anticrossing, characterized by probabilities $D = \exp(-2\pi\gamma)$ and $A = 1 - D$ for diabatic and adiabatic transitions, respectively. The model assumes a core with one nonvanishing quantum defect μ_0 and with extremal Stark-level slopes, so that $\gamma = |\mu_0|^2/3Fn^{10}$ for all anticrossings, where the manifolds have principal quantum numbers n and $n + 1$. Interference effects are ignored, which allows analytical treatment of the system's evolution using path statistics or recursion relations. An initially populated edge state leads to a single-humped distribution of level populations. Analytical expressions are found for the probability distribution as a function of time, as well as its average and standard deviation. Limiting forms of the distribution at large times and in the diabatic ($D \rightarrow 1$) and adiabatic ($D \rightarrow 0$) limits are also given. These features are contrasted with those of a random walk. The relevance of the model to selective-field ionization is discussed.

PACS number(s): 32.80.Bx, 32.60.+i, 32.90.+a

I. INTRODUCTION

Atomic Rydberg levels split in the presence of electromagnetic fields and undergo shifts whose magnitudes generally increase with field amplitude. Familiar examples include the Stark and diamagnetic Zeeman spectra in static fields \mathbf{F} and \mathbf{B} and quasienergy spectra in monochromatic ac fields [1]. It is common for entire manifolds of levels to suffer such large shifts that, when atom-field interactions exceed Rydberg-level spacings, manifolds overlap (see Fig. 1). The coupling of states by the atomic core plus the *dynamical* coupling induced by variations of the fields in time may lead to complex behavior in the time evolution of the system. The interaction of two or even several manifolds—forming a grid of many avoided crossings that may vary in size (some may even appear vanishingly small) [2,3]—makes the prediction of time evolution particularly vexing. Much work on time-dependent forces has been inspired by the ubiquity of multiple-level crossings in atomic and molecular collision processes [4]. A more pertinent example to Rydberg-atom physics is that of selective-field ionization [5] (SFI): In response to rapid, monotonic variations in the amplitude of an external electric field, the distribution of level populations evolves in time, usually nonadiabatically, leading eventually to ionization. The evolution of the state of the system may be described as the collective tracing in time of a set of pathways, each involving a series of adiabatic and nonadiabatic transitions among anticrossing levels.

In lieu of a brute-force numerical solution of the time-dependent Schrödinger equation incorporating a large

basis of Rydberg states, clues to basic features of the time evolution can be obtained by considering simplified models. We take such an approach here in an initial attempt to characterize the history of two coupled Rydberg manifolds under the influence of a linearly ramped electric field $F(t) = \dot{F}t$. The two-manifold grid shown in Fig. 2 is

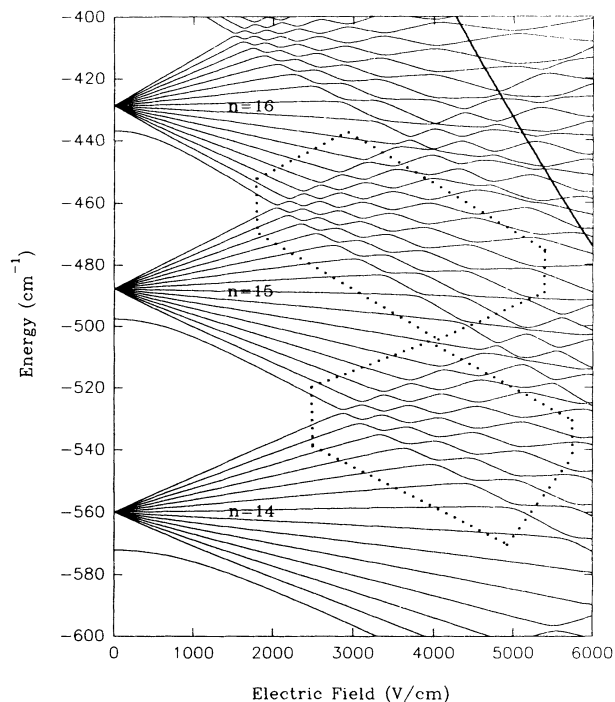


FIG. 1. Stark map of $m_l=0$ Rydberg levels vs. electric field for manifolds $n = 14-16$. Quantum defects chosen as $\mu_0=0.15$, $\{\mu_l=0, l > 0\}$, to illustrate individual avoided crossings. The dotted lines indicate regions where nearly parallel diabatic levels from the $n = 15$ manifold cross only those of either adjacent manifold. The classical ionization limit, curve at upper right. (Figure courtesy K. B. MacAdam.)

*Present address: Indoor Environment Program, Building 90, Room 3058, Lawrence Berkeley Laboratory, Berkeley, CA 94720.

the model for the manifold-crossing regions indicated on the Stark map of Fig. 1. We invoke the Landau-Zener (LZ) approximation [6,7] and assume that (i) all transitions between states of different manifolds occur at distinct, isolated pairwise anticrossings of adiabatic levels and (ii) transitions do not occur between states of the same manifold. The further assumption (iii) that intramanifold levels are parallel is motivated by the observation that neighboring manifolds (Fig. 1) first encounter one another through their few extremal levels, whose slopes do not differ greatly in magnitude. Second-order Stark shifts are small and in any case do not contribute to the main features of the intermanifold interactions, so we will neglect them and assume *constant* slopes. We also make the ostensibly severe approximation of (iv) ignoring interference effects among different paths. The purpose here, however, is to allow us to identify *average* population distributions upon traversing a great many avoided crossings. The inclusion of interference in the model has been investigated separately [8] and will be reported elsewhere. The distribution we obtain for *incoherent* evolution will prove interesting in its own right as a new variant of the familiar random walk.

In a uniform electric field $\mathbf{F}(t)=F(t)\hat{\mathbf{z}}$, m_l is a good quantum number and an n manifold consists of $n-|m_l|$ Rydberg levels. We consider here only $m_l=0$. At small fields, the high- l (i.e., most) members of each manifold are nearly degenerate, and the eigenstates composed of mixtures within this subset suffer linear energy shifts ($\propto F$) that form a pseudohydrogenic Stark fan [3]; the few low- l states having appreciable quantum defects $\{\mu_l\}$ [9] shift only quadratically. Let $|\mu|$ be the largest value $|\mu_l \pmod{1}|$ [9]. At larger fields, such that $F \geq \frac{2}{3}|\mu|n^{-5}$ all spherical states are ultimately mixed by the field into a linearly split manifold whose eigenstates are closely approximated by hydrogen-Stark eigenstates $|nn_1n_2m_l\rangle$ [10]. State mixing in the single-manifold regime has been studied in some detail for the case of linearly ramped fields [11].

The rationale for our model of a LZ grid stems from the structure of the atomic Hamiltonian in the crossing regime, $F \geq \frac{1}{3}(n \pm \frac{1}{2})^{-5}$. Within the subspace of each manifold of states, the Hamiltonian is similar to that of hydrogen. The linear hydrogenic Stark splitting,

$$E_{nn_1n_20}(F) = -\frac{1}{2}n^{-2} + \frac{3}{2}Fn(n_1 - n_2) + O(F_2n^6) \quad (1)$$

(all quantities are in atomic units), becomes so large that one manifold's levels begin to cross with and couple significantly to those of its neighbors ($n'=n \pm 1$). The field-independent coupling, provided by the core, between states of any manifolds n' and n (including $n'=n$) is given by the Hamiltonian matrix elements [3,11]

$$\begin{aligned} v_{n'n'_10,nn_10} &= \langle n'n'_1n'_20 | H_{\text{core}} | nn_1n_20 \rangle \\ &= -(n'n)^{-2} \sum_{l=0}^n \mu_l u_{n'_1l}^{(n'0)} u_{n_1l}^{(n0)}, \end{aligned} \quad (2)$$

where $n^{-1/2}u_{n_1l}^{(n0)}$ and its primed partner are coefficients of the linear transformation between zero-field hydrogenic eigenstates (of the same manifold, for $m_l=0$) of para-

bolic and spherical symmetry [12]. When the block of intramanifold ($n'=n, m_l=0$) elements (2) is dominated by the diagonal atom-field interaction (1), the eigenstates within each block are, to first order,

$$\begin{aligned} |nq0\rangle &\approx |nn_1n_20\rangle \\ &+ \frac{1}{3Fn^5} \sum_{n'_1 \neq n_1}^{n-1} \sum_{l=0}^{n-1} \mu_l \frac{u_{n'_1l}^{(n'0)} u_{n_1l}^{(n0)}}{n_1 - n'_1} |nn'_1n'_20\rangle \\ &+ O\left[\left(\frac{|\mu|}{Fn^5}\right)^2\right]. \end{aligned} \quad (3)$$

[Each eigenstate label $q=0, \dots, (n-1)$ may be identified with the parabolic quantum number $n_1=0, \dots, (n-1)$ of its dominant hydrogenic component $|nn_1n_20\rangle$.] Prediagonalization of the Hamiltonian within each manifold via the basis (3) then leads to adiabatic levels [10,11]

$$\begin{aligned} E_{nq0}(F) &= -\frac{1}{2}n^{-2} + \frac{3}{2}Fn(n_1 - n_2) - n^{-4} \sum_{l=0}^{n-1} \mu_l [u_{n_1l}^{(n0)}]^2 \\ &+ O\left[\frac{|\mu|^2}{Fn^9}\right], \end{aligned} \quad (4)$$

which, to first order, differ from the hydrogenic levels (1) at large F only by constant shifts. The core coupling between prediagonalized states of different manifolds is now given by Eq. (2) (with $n' \neq n$), plus terms of higher order in $2|\mu|/3Fn^5$ and $2|\mu|/3Fn^5$.

The *dynamical* coupling among states of the same n manifold, i.e., within the basis (3) and induced by the time dependence of $F(t)$, is shown in Ref. [11] to decrease as F^{-2} when $F \gg 2|\mu|/3n^5$. The ratio of its magnitude to that of the core coupling

$$|v_{n'n'_10,nn_10}| \sim |\mu|n^{-4}$$

[Eq. (2)] is then of the order of $\dot{F}n^4/|\mu|^2$ or smaller, which is negligible except in the limit of extraordinarily high ramp rates \dot{F} . The dynamical Stark coupling of hydrogenic levels of different manifolds is a few orders of magnitude smaller than the core coupling and can also be neglected [13].

As long as $|\mu|$ is not close to $\frac{1}{2}$, the atom's adiabatic Hamiltonian in the crossing region $F \geq \frac{1}{3}(n + \frac{1}{2})^{-5}$ reduces, therefore, to shifted hydrogenic levels for n and $n'=n+1$, coupled to lowest order by the matrix elements of Eq. (2). The coupling between $|nn_1n_20\rangle$ and $|n'n'_1n'_20\rangle$ produces an energy gap—an avoided crossing—of width $|2v_{n'n'_1n_1}| \sim 2|\mu|n^{-4}$ [3,14]:

$$|2v_{n'n'_1n_1}| = 2(n'n)^{-2} \left| \sum_{l=0}^n \mu_l u_{n'_1l}^{(n'0)} u_{n_1l}^{(n0)} \right| \quad (5)$$

(we have dropped from v the manifold indices n' and n , and $m_l=0$). When $F \approx \frac{1}{3}n^{-5}$, the gaps are a fraction $\sim 2|\mu|$ of the splittings [15] $3Fn \approx n^{-4}$, so we must assume that $|\mu| \ll \frac{1}{2}$ in this model. Pairs of levels then mix appreciably only when their energies differ by less than

the intramanifold splitting, and it is in this sense that the anticrossings may be considered "isolated." The first and subsequent avoided crossings at $F \gtrsim \frac{1}{3}(n + \frac{1}{2})^{-5}$ involve the upward- and downward-going levels at the edges of manifolds n ($n_1 = n - 1$, $n_2 = 0$) and $n' = n + 1$ ($n'_1 = 0$, $n'_2 = n' - 1$), respectively, and neighboring levels. Their extremal diabatic slopes,

$$p = \frac{dE_{n_1 n_2 0}}{dt} = \frac{3}{2} \dot{F} n (n - 1), \quad (6)$$

$$p' = \frac{dE_{n'_1 n'_2 0}}{dt} = -\frac{3}{2} \dot{F} n (n + 1),$$

are nearly equal and opposite, and serve to approximate the slopes of all crossing diabatic levels. ["Diabatic" refers here to the *noninteracting*, nonhydrogenic levels (4).] These remarks justify the assumptions (i), (ii), and (iii) made above.

The Landau-Zener problem [4,6,7] for each isolated two-level interaction depends only on the gap sizes in Eq. (5) and on the difference of the slopes in Eq. (6). (Note that the condition $2|\mu| \ll 1$ for small gaps also implies that the time between successive avoided crossings is sufficiently longer than the LZ transition time [16] for the transition to be "complete.") The probability of a diabatic (i.e., nonadiabatic) transition in the LZ model is

$$D_{n'_1 n_1}(\dot{F}) = \exp(-2\pi\gamma_{n'_1 n_1}), \quad \gamma_{n'_1 n_1} = \frac{|v_{n'_1 n_1}|^2}{|p - p'|}. \quad (7)$$

In keeping with a simple model, we will further take $v_{n'_1 n_1} \equiv v$ to be the same for every intersection; this is equivalent to assuming that $\mu_l = 0$ for $l > 0$, since the s state couples all n_1 states equally [11]: $u_{n_1 0}^{(n)} = 1$. Then $\mu = \mu_0$ and Eqs. (5)–(7) evaluate to $|2v| = 2|\mu_0|n^{-4}$, $|p - p'| = 3\dot{F}n^2$, and

$$D(\dot{F}) = \exp(-2\pi\gamma), \quad \gamma = \frac{v^2}{|p - p'|} = \frac{|\mu|^2}{3\dot{F}n^{10}}, \quad (8)$$

which has the same value for every anticrossing, as does the probability of an adiabatic transition, $A \equiv 1 - D$.

In Sec. II we delineate the topology of the two-manifold model, for which the time evolution is derived statistically in Sec. III. We characterize the resulting single-humped distribution of level populations in Sec. IV by its average position and spread among the levels. In Sec. V we present an alternative method for describing the evolution, based on 2×2 matrices. We conclude in Sec. VI with a discussion of some refinements to the model.

II. THE TWO-MANIFOLD MODEL

Consider two intersecting manifolds of parallel energy levels, E_m and $E_{m'}$. Within each manifold the levels vary linearly in time with slope $p = dE/dt$ or $p' < p$ [Eq. (6)] and have constant separation $\epsilon = 3Fn$ or $\epsilon' = 3Fn'$:

$$E_m(t) = pt - m\epsilon, \quad E_{m'}(t) = p't + m'\epsilon'. \quad (9)$$

The upward-going levels E_m are numbered

$m = 0, 1, 2, \dots$ from the top down, while the downward-going ones $E_{m'}$ are labeled $m' = 0', 1', 2', \dots$ from the bottom up. (The indices m and m' should not be confused with m_l .) Since the addition of the same energy $p''t$ (any p'') to all levels makes no physical difference, we are free to adjust the slopes so that $p \approx 3\dot{F}n^2 > 0$ and $p' = -p < 0$. In the absence of interactions between the manifolds, each pair of levels would intersect at the point

$$t_{mm'} = \frac{m\epsilon + m'\epsilon'}{p - p'}, \quad (10)$$

$$E_{mm'} = \frac{pm'\epsilon' + p'm\epsilon}{p - p'}, \quad (11)$$

which we label $[m, m']$. The energy and times scales [and hence the field $F(t) = \dot{F}t$] have been implicitly shifted from those of Sec. I so that, as time increases, the first such intersection, $[0, 0']$, occurs at the origin of (t, E) . Subsequent intersections at $t > 0$ form a grid that is confined to the range $-pt \leq E \leq pt$ between levels 0 and $0'$ and whose nodes are in general skewed in time.

Insofar as the levels evolve adiabatically between intersections and undergo transitions from one manifold to the other only in the vicinity of level (anti)crossings "at" the intersections, the time evolution of the system depends only on the *topology* of the network, i.e., on the connections among the various intersections $[m, m']$. We may therefore assume that the levels of both manifolds are equally spaced, $\epsilon' = \epsilon \approx n^{-4}$, so that the grid is symmetric about $E = 0$:

$$E_m(t) = pt - m\epsilon, \quad E_{m'}(t) = -pt + m'\epsilon. \quad (12)$$

The N th "generation" of $N + 1$ level crossings $[m, m']$ is then grouped according to

$$N = m + m' = 0, 1, 2, \dots, \quad (13)$$

which serves to identify a particular manifold-interaction time (10),

$$t^{(N)} = \frac{1}{2}N\epsilon/p, \quad (14)$$

as well as to label that generation's intersection energies (11),

$$E_{mm'}^{(N)} = \frac{1}{2}(m' - m)\epsilon, \quad \frac{1}{2}N\epsilon \geq E_{mm'}^{(N)} \geq -\frac{1}{2}N\epsilon. \quad (15)$$

We begin generation numbering at $[0, 0']$ with $N = 0$ in order to associate the probability of arriving "at" intersection $[m, m']$ with the number N of *prior* intersections. The adiabatic segment of level $E_m(t)$ [or $E_{m'}(t)$] spanning intersection times $t^{(N-1)}$ and $t^{(N)}$ will be labeled $m^{(N)}$ [or $m'^{(N)}$].

We specify the initial condition that all population at $t < 0$ resides in the upward-going level 0. A "path" through the grid can then be represented in several ways: (1) As a sequence of adjacent intersections for $N = 0, 1, 2, \dots$; (2) as a sequence of adiabatic segments $m^{(N)}$ and $m'^{(N)}$ for $N = 0, 1, 2, \dots$; and (3) more simply, as a string of arrows \uparrow and \downarrow , either $\{\uparrow: \uparrow \dots\}$ or $\{\uparrow: \downarrow \dots\}$, indicating successive steps up or down in energy; the string begins with " \uparrow :" for the initial step-up approach to $[0, 0']$, followed in turn by steps approaching

where $A = 1 - D$ and the sum is over all $k \geq 0$ such that neither binomial coefficient vanishes. The derivation for paths that end with a \downarrow is similar, but involves an odd number $2k - 1$ of adiabatic transitions ($1 \leq 2k - 1 \leq N$), with pairs of A 's separated by $k - 1$ blocks of \downarrow 's plus one A preceding the final string of \downarrow 's ending at $[m, m']$. The total probability for arriving at $[m, m']$ on the downward-going segment $m'^{(N)}$ is [18]

$$P_{mm'\downarrow}^{(N)}(D) = \delta_{m, N-m'} \sum_k \binom{m-1}{k-1} \binom{m'}{k-1} A^{2k-1} D^{N-2k+1}, \quad (17)$$

with $k \geq 1$.

The distribution (16) generally does not exhibit any particular symmetry at fixed N for arbitrary D . One can only say that $P_{N0\uparrow}^{(N)}(D) = 0$ always holds for $N > 0$, since level $0'$ can only be reached by a \downarrow ; similarly, $P_{0N'\downarrow}^{(N)}(D) = 0$ for the purely diabatic path. However, the

$$P_{mm'}^{(N)}(D) = \delta_{m+m', N} \sum_k \binom{m-1}{k-1} \left[\binom{m'}{k} A^{2k} D^{N-2k} + \binom{m'}{k-1} A^{2k-1} D^{N-2k+1} \right], \quad (19)$$

where $k \geq 0$ ranges over all nontrivial values, with the proviso that $\binom{-1}{1} \equiv 1$. It is assumed that the various paths leading up to each $[m, m']$ have made transitions through N previous intersections but have not yet undergone the LZ transition at $[m, m']$. Equivalently, Eq. (19) is the total (conserved) probability of passing through the intersection $[m, m']$ onto the level segments $m^{(N+1)}$ and $m'^{(N+1)}$.

$$\begin{aligned} P_{mm'}^{(N)}(D) &= P_{mm'\uparrow}^{(N)}(D) + P_{mm'\downarrow}^{(N)}(D) \\ &= P_{m, m'+1, \uparrow}^{(N+1)}(D) + P_{m+1, m', \downarrow}^{(N+1)}(D), \end{aligned} \quad (20)$$

which is perhaps a more apt operational definition. An immediate consequence of Eqs. (18) and (20) for a midgrid intersection $[m, m]$ is

$$P_{mm'}^{(N)}(D) = P_{m, m'-1}^{(N-1)}(D), \quad m' = m. \quad (21)$$

This result applies to adjacent intersections, for $N - 1$ and N , that lie on the purely adiabatic path, with N even and $m = \frac{1}{2}N$.

Table I shows the polynomials $P_{mm'\uparrow}^{(N)}(D)$ and $P_{mm'\downarrow}^{(N)}(D)$ as functions of D and A up to $N = 6$. Note that the number of all paths arriving at $[m, m']$ with positive slope, i.e., along $m^{(N)}$, is given by the sum (16) for $D = A = \frac{1}{2}$,

$$2^N P_{mm'\uparrow}^{(N)}\left(\frac{1}{2}\right) = \binom{N-1}{m} = \frac{(N-1)!}{m!(m'-1)!}, \quad (22a)$$

the number of all paths arriving with negative slope [along $m'^{(N)}$] is given by the sum (17),

$$2^N P_{mm'\downarrow}^{(N)}\left(\frac{1}{2}\right) = \binom{N-1}{m'} = \frac{(N-1)!}{(m-1)!m'!}, \quad (22b)$$

and their total in Eq. (19) is, of course, $N!/(m!m'!)$, just as it would be for a random walk.

distribution $P_{mm'\downarrow}^{(N)}(D)$ is always symmetric at fixed N about the center of the subset of levels $1 \leq m \leq N$:

$$P_{mm'\downarrow}^{(N)}(D) = P_{m'+1, m-1, \downarrow}^{(N)}(D). \quad (18)$$

This invariance follows from the joint substitution $\{m \rightarrow m'+1, m' \rightarrow m-1\}$ in Eq. (17), which leaves $m + m'$ unchanged. Neither $P_{mm'\uparrow}^{(N)}(D)$ nor $P_{mm'\downarrow}^{(N)}(D)$ is invariant under the operation $m \leftrightarrow m'$ for $N > 0$, so they are not symmetric about the center of the grid.

The initial population $P_{00'\uparrow}^{(0)} = 1$ will in time become redistributed among m and m' levels over the breadth of the grid according to $P_{mm'\uparrow}^{(N)}(D)$ and $P_{mm'\downarrow}^{(N)}(D)$. To characterize the distribution over energy as a function of time, we consider the probability for arriving at N th-generation intersection points $(t^{(N)}, E_{mm'}^{(N)})$, Eqs. (14)–(15), along either adiabatic energy-level segment approaching $[m, m']$, i.e., along $m^{(N)}$ or $m'^{(N)}$. This quantity is the sum of Eqs. (16)–(17):

Figure 3 shows the total populations (19) as histograms on a two-dimensional grid of m' vs m for various values of D between 1 and 0. These maps cover generations $N = 0$ through $N = 32$; $[0, 0']$ lies at the rear corner and time sweeps forward in steps (14) marked by diagonals of constant $m + m' = N$. During the fastest ramps ($\gamma \approx 0$, $D \approx 1$), population leaks off to other levels but clings to the original $m = 0$ level with probability

$$\begin{aligned} D^N &= \exp(-2\pi\gamma N) = \exp\left[-\frac{4\pi\gamma p}{\epsilon} t\right] \\ &= \exp\left[-\frac{2\pi v^2}{\epsilon} t\right], \end{aligned} \quad (23)$$

where we have set $t^{(N)} = t$ and where $v = -\mu_0 n^{-4}$ is the intermanifold level coupling (2) in Eq. (8). The initial level decays exponentially to a quasicontinuum of m' levels, as in Demkov's model [19] for one level crossing many. [Equation (23) results here even if interference between paths is not ignored.] During the slowest ramps ($A \approx 1$), on the other hand, population tends to favor the purely adiabatic path and paths near it, which remain near the center of the interaction region, $m \approx m'$. The random-walk case $D = A = \frac{1}{2}$ leads to a distribution $P_{mm'}^{(N)}(\frac{1}{2})$ that is precisely symmetric in $m \leftrightarrow m'$ (cf. Table 1), converging to a Gaussian at high N with full width $\sqrt{N} \epsilon$ in energy.

IV. POPULATION AVERAGE AND SPREAD

The feature common to the distributions $P_{mm'}^{(N)}(D)$ shown in Fig. 3 is the appearance of a single hump at all times (i.e., for all N) and for all values of D . The hump is, moreover, almost always centered near $m \approx m'$. Even for fast ramps, when the population persists in being skewed towards the initial $m = 0$ level, $P_{mm'}^{(N)}(D)$ will eventually

shift its center towards the grid's center at high enough N . The *width* of the hump scales with D as expected: It is narrower the more nearly adiabatic is the evolution ($A \rightarrow 1$, $D \rightarrow 0$), and broad for predominantly nonadiabatic evolution ($D > A$). Because the redistribution of probability for any one time step is a Markovian process— independent of all previous time steps—the position and width of the hump are easily calculated as follows.

The upward-going level \uparrow approaching any one avoided crossing $[m, m']$ has probability D (or A) of passing through to the next \uparrow (or down to the next \downarrow), thereby increasing (or decreasing) its energy (15) by $+\frac{1}{2}\epsilon$ (or $-\frac{1}{2}\epsilon$) at the next intersection. A downward-going level \downarrow has

TABLE I. Up- and down-going level populations [Eqs. (16) and (17)] for initially populated \uparrow level $0^{(0)}$ vs. intersections $[m, m']$ for $N=0-6$. The sum of the two columns is $P_{mm'}^{(N)}(D)$, Eq. (19). Note $A=1-D$ and $m+m'=N$.

$[m, m']$	$P_{mm'\uparrow}^{(N)}(D)$	$P_{mm'\downarrow}^{(N)}(D)$
	$N=0$	
$[0, 0']$	1	0
	$N=1$	
$[0, 1']$	D	0
$[1, 0']$	0	A
	$N=2$	
$[0, 2']$	D^2	0
$[1, 1']$	A^2	DA
$[2, 0']$	0	DA
	$N=3$	
$[0, 3']$	D^3	0
$[1, 2']$	$2DA^2$	D^2A
$[2, 1']$	DA^2	$D^2A + A^3$
$[3, 0']$	0	D^2A
	$N=4$	
$[0, 4']$	D^4	0
$[1, 3']$	$3D^2A^2$	D^3A
$[2, 2']$	$2D^2A^2 + A^4$	$D^3A + 2DA^3$
$[3, 1']$	D^2A^2	$D^3A + 3D^2A^3$
$[4, 0']$	0	D^3A
	$N=5$	
$[0, 5']$	D^5	0
$[1, 4']$	$4D^3A^2$	D^4A
$[2, 3']$	$3D^3A^2 + 3DA^4$	$D^4A + 3D^2A^3$
$[3, 2']$	$2D^3A^2 + 2DA^4$	$D^4A + 4D^2A^3 + A^5$
$[4, 1']$	D^3A^2	$D^4A + 3D^2A^3$
$[5, 0']$	0	D^4A
	$N=6$	
$[0, 6']$	D^6	0
$[1, 5']$	$5D^4A^2$	D^5A
$[2, 4']$	$4D^4A^2 + 6D^2A^4$	$D^5A + 4D^3A^3$
$[3, 3']$	$3D^4A^2 + 6D^2A^4 + A^6$	$D^5A + 6D^3A^3 + 3DA^5$
$[4, 2']$	$2D^4A^2 + 3D^2A^4$	$D^5A + 6D^3A^3 + 3DA^5$
$[5, 1']$	D^4A^2	$D^5A + 4D^3A^3$
$[6, 0']$	0	D^5A

instead probability A (or D) for changing its energy by $+\frac{1}{2}\epsilon$ (or $-\frac{1}{2}\epsilon$). The average energy shift per intersection is thus $\pm(D-A)\frac{1}{2}\epsilon$ for initial levels with slope $\pm p$.

It is convenient to introduce the index

$$\mu \equiv m' - m = E_{mm'}^{(N)} / \frac{1}{2}\epsilon, \quad (24)$$

which is an intersection energy in units of $\frac{1}{2}\epsilon$. This rescales the time-energy grid coordinates (14)–(15) to

$$(N, \mu) = (m' + m, m' - m)$$

by rotating the axes by 45° —parallel to the lattice. Note that μ ranges from $-N$ to N in steps of 2.

Consider now the \uparrow level segment $m^{(N)}$ approaching an arbitrary intersection $[m, (N-m)']$. Suppose that, after passing through I subsequent intersections ($I \geq 1$), the rescaled energy shifts on the average by some amount $\bar{\mu}_I$ relative to the initial value $\mu = N - 2m$. An initial \downarrow level segment $m^{(N)}$ approaching some $[(N-m)', m']$ will likewise suffer an equal and opposite average shift $-\bar{\mu}_I$ after I subsequent intersections, due to the up-down symmetry of the grid. In particular, the \uparrow level $0^{(1)}$ will suffer an average shift $\bar{\mu}_{N-1}$, relative to the value $\mu = +1$ at $[0, 1']$, after passing through $I = N - 1$ more anticrossings at times $t^{(1)}, \dots, t^{(N-1)}$; the \downarrow level $0^{(1)}$ will suffer an average shift $-\bar{\mu}_{N-1}$ relative to the value $\mu = -1$ at $[1, 0']$. With respect to the \uparrow level $0^{(0)}$ approaching the *very first* intersection, the average μ shift after N intersections is

$$\begin{aligned} \bar{\mu}_N &= D[1 + \bar{\mu}_{N-1}] + A[-1 - \bar{\mu}_{N-1}] \\ &= \delta[1 + \bar{\mu}_{N-1}], \end{aligned} \quad (25)$$

where

$$\delta \equiv D - A = 2D - 1, \quad -1 \leq \delta \leq 1 \quad (26)$$

measures the average size of the μ step. Since $E = E_{00'}^{(0)}$ and $\mu = 0$ at $[0, 0']$, one seeds the recursion relation (25) with $\bar{\mu}_0 = 0$. The average value of μ after N generations then equals [17]

$$\bar{\mu}_N(\delta) = \sum_{\mu=-N}^N P_{mm'}^{(N)}(D)\mu = \sum_{j=1}^N \delta^j = \frac{\delta(1-\delta^N)}{1-\delta}, \quad (27)$$

where $D = \frac{1}{2}(1 + \delta)$. The average *energy* at $t^{(N)}$ is

$$\bar{E}^{(N)}(D) = \frac{1}{2}\epsilon \bar{\mu}_N(2D - 1).$$

To obtain the standard deviation of μ , one needs to find $\overline{\mu_N^2}$. If one knows both $\bar{\mu}_I$ and $\overline{\mu_I^2}$ for an initial \uparrow that passes through I intersections, then shifting all values of μ by $+1$ yields a new average,

$$\overline{(\mu+1)^2} = \overline{\mu^2} + 2\bar{\mu} + 1. \quad (28)$$

An initial \downarrow , with μ shifted down by -1 , again yields the right-hand side of Eq. (28), since $(-\mu-1)^2 = (\mu+1)^2$. Now repeat the steps leading to Eq. (25): approach $[0, 0']$ on the \uparrow level $0^{(0)}$, and branch off to $[0, 1']$ and $[1, 0']$ with probabilities D and A , respectively. There follows

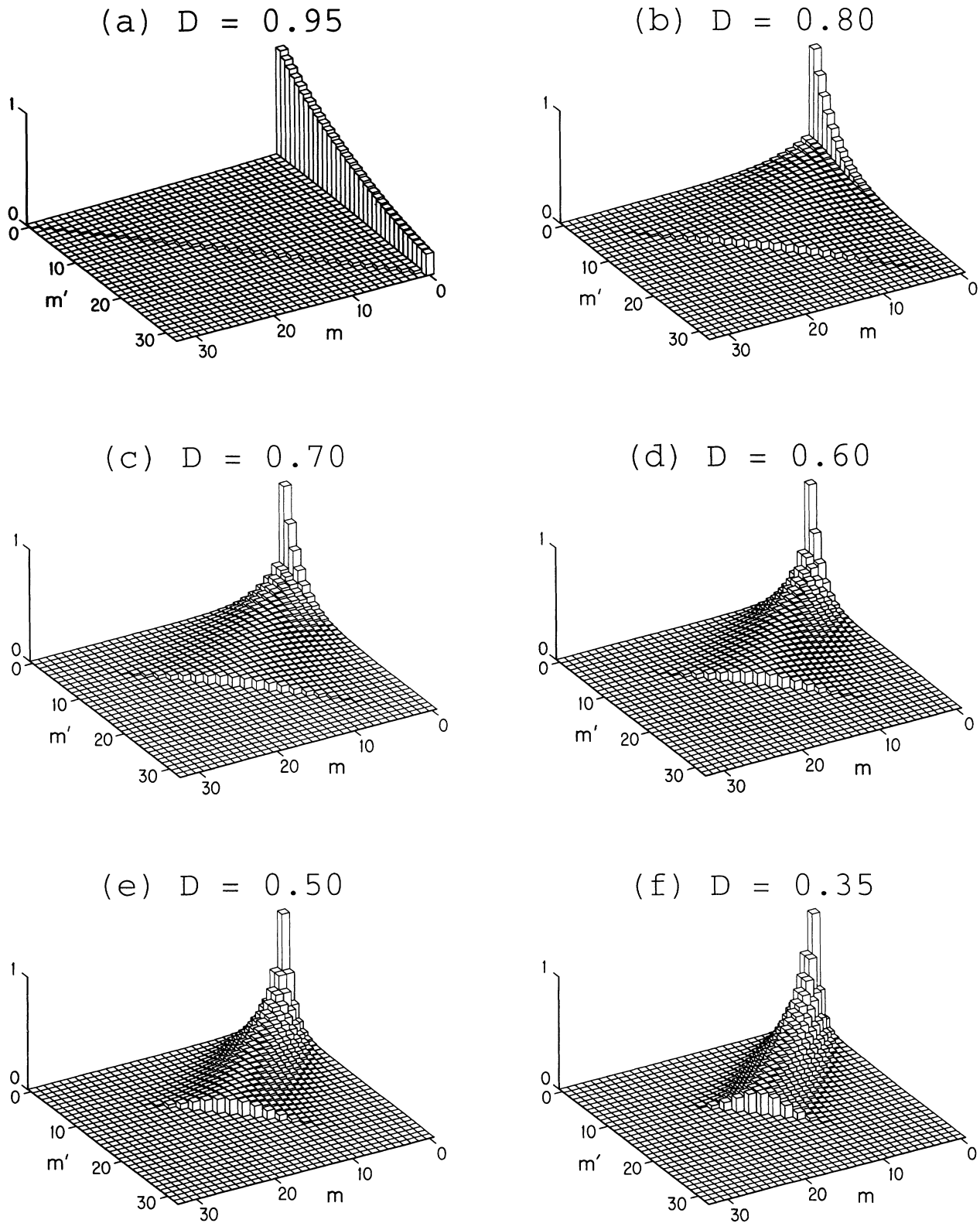


FIG. 3. Probability $P_{mm'}^{(N)}(D)$ [from Eq. (19) or Eq. (40)] of arriving at intersection $[m, m']$ on either an \uparrow or \downarrow level, on a Landau-Zener grid with $N = m + m' = 0-32$. Time values $t^{(N)}$ marked by diagonals of constant $N = m + m'$ [$t^{(0)} = 0$ lies at rear corner]. The initial level is \uparrow , $m = 0$; the histogram at $[0, 0']$ has unit height. The values of diabatic-transition probabilities D used are as follows: (a) 0.95, (b) 0.80, (c) 0.70, (d) 0.60, (e) 0.50, (f) 0.35, (g) 0.20, and (h) 0.05. Note exponential leakage [Eq. (23)] from initial $m = 0$ for large D in (a) and (b), narrower large- N widths for smaller D , and dominance of the purely adiabatic path for $D \approx 0$ in (h). Case (e) alone is equivalent to a random walk.

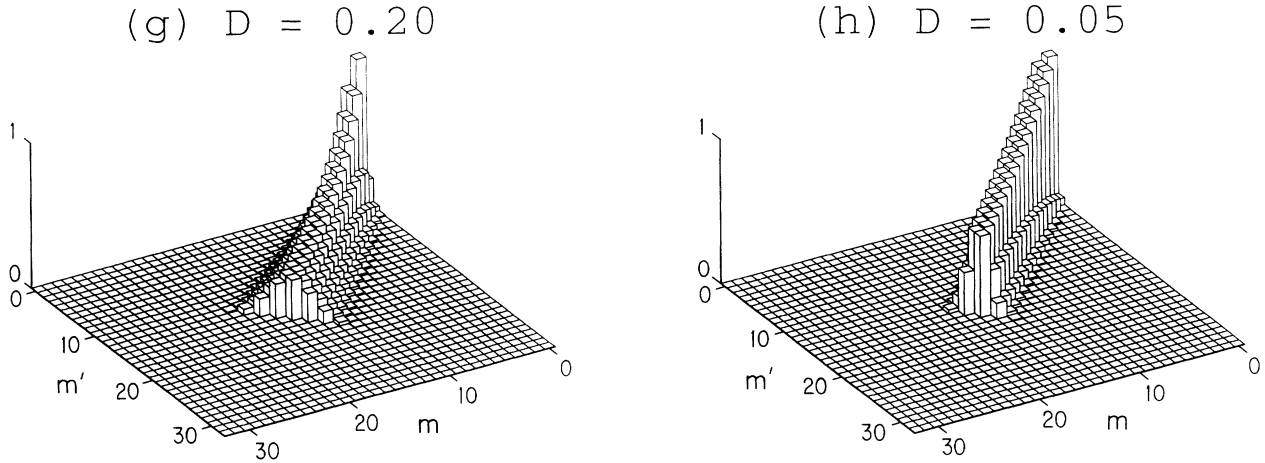


FIG. 3. (Continued).

the recursion relation

$$\begin{aligned} \overline{\mu_N^2} &= D [1 + 2\overline{\mu_{N-1}} + \overline{\mu_{N-1}^2}] + A [1 + 2\overline{\mu_{N-1}} + \overline{\mu_{N-1}^2}] \\ &= 1 + 2 \sum_{j=1}^{N-1} \delta^j + \overline{\mu_{N-1}^2}, \end{aligned} \tag{29}$$

where we have used $D + A = 1$ and Eq. (27). Seed Eq. (29) with $\overline{\mu_0^2} = 0$ to obtain

$$\begin{aligned} \overline{\mu_N^2}(\delta) &= N + 2 \sum_{j=1}^{N-1} \sum_{k=1}^j \delta^k \\ &= \left[\frac{1+\delta}{1-\delta} \right] N - \frac{2}{1-\delta} \overline{\mu_N}(\delta). \end{aligned} \tag{30}$$

Finally, the standard deviation (half width) in μ at generation N is

$$\begin{aligned} \Delta\mu_N(\delta) &= \left[\left[\frac{1+\delta}{1-\delta} \right] N - \frac{2}{1-\delta} \overline{\mu_N}(\delta) - \{ \overline{\mu_N}(\delta) \}^2 \right]^{1/2} \\ &= \left[\left[\frac{1+\delta}{1-\delta} \right] N - \frac{\delta(1-\delta^N)(2+\delta-\delta^{N+1})}{(1-\delta)^2} \right]^{1/2}. \end{aligned} \tag{31}$$

In energy units, the full width of $P_{mm'}^{(N)}(D)$ at $t^{(N)}$ is just

$$\Gamma^{(N)}(D) = \epsilon \Delta\mu_N(2D - 1).$$

The average value of $m' - m$ for the distribution $P_{mm'}^{(N)}(D)$, Eq. (27), is not simply proportional to N . This stands in contrast to a generic one-dimensional random walk, where the average displacement from the starting point varies linearly with the number of steps taken if the probabilities of stepping up and down are not equal. On the other hand, the standard deviation, Eq. (31), does scale like \sqrt{N} at large N . If and only if $D = A$ ($\delta = 0$) do we recover precisely the random-walk results

$$\overline{\mu_N}(0) = 0 \text{ and } \Delta\mu_N(0) = \sqrt{N} \tag{32}$$

at all N .

To evaluate $\overline{\mu_N}(\delta)$ and $\Delta\mu_N(\delta)$ in various other limits, note first that if $A > D$, then $\delta < 0$ and we must replace δ

by $-|\delta|$ in the above formulas. Terms $|\delta|^N$ will be much smaller than unity unless $|\delta| \approx 1$, i.e., unless $\delta = 1 - 2A \leq 1$ when $A \approx 0$ (adiabatic limit) or $\delta = 2D - 1 \geq -1$ when $D \approx 0$ (adiabatic limit). The condition $|\delta|^N \ll 1$ is then satisfied for $N \gg 1/2A$ when $D \rightarrow 1$ and for $N \gg 1/2D$ when $A \rightarrow 1$. Similarly, neglecting the second term under the square root on the second line of Eq. (31) requires

$$N \gg \left| \frac{2\delta}{1-\delta^2} \right| = \left| \frac{1}{2A} - \frac{1}{2D} \right|, \tag{33}$$

the same constraint for "large N ."

In the limit (33), the single hump of $P_{mm'}^{(N)}(D)$ is thus characterized by

$$\begin{aligned} \overline{\mu_N}(\delta) \pm \Delta\mu_N(\delta) &\rightarrow \frac{\delta}{1-\delta} \pm \left[\frac{1+\delta}{1-\delta} N \right]^{1/2} \\ &= \frac{D-A}{2A} \pm \left[\frac{D}{A} N \right]^{1/2}, \text{ fixed } \delta. \end{aligned} \tag{34}$$

Note that $\overline{\mu_N}(\delta)$ and $\Delta\mu_N(\delta)$ approach the limiting values (34) exponentially. In the large- N adiabatic limit $1 \gg D \gg 1/2N$, the width becomes very narrow in energy:

$$\Gamma^{(N)}(D) \xrightarrow{D \rightarrow 0} \epsilon \sqrt{DN}.$$

The high probability of paths following adiabatic turns at most intersections works against diffusion in energy and thus provides a kind of stabilization of the energy. However, the width in the large- N adiabatic limit $1 \gg A \gg 1/2N$ can be quite broad:

$$\Gamma^{(N)}(D) \xrightarrow{A \rightarrow 0} \epsilon \sqrt{N/A}.$$

This results from the tendency of paths dominated by adiabatic transitions to continue unidirectionally in energy and thereby remain diffuse over many generations.

The average level position $\overline{\mu_N}(\delta)$ is also lopsided in its adiabatic vs. diabatic behavior. Faster ramps ($\delta \rightarrow 1$) lead to the asymptotic shift $\delta/(1-\delta) \rightarrow 1/2A$, which

may be large but is ultimately *constant*. Thus, the outcome of a fast ramp applied to the $m=0$ level is leakage off the initial path along $E_0(t)=pt$, according to Eq. (23), to a mean asymptotic energy $E=\bar{E}^{(N)}(D) \rightarrow \frac{1}{4}\epsilon/A$, accompanied by a severe broadening about this energy. Slower ramps ($-1 \leq \delta < 0$), on the other hand, attain distributions shifted to positions

$$\bar{\mu}_N(\delta) = -|\delta|/(1+|\delta|),$$

which always lie between $\mu = -\frac{1}{2}$ and 0, and sport widths smaller than \sqrt{N} . In fact, the purely adiabatic path ($\delta = -1$) oscillates between $\mu = -1$ and 0 as N alternates between odd and even values, respectively: Compare the *average* value obtained from Eq. (34) in the extreme adiabatic case, $\bar{\mu}_N(-1) = -\frac{1}{2}$ [i.e., $\bar{E}^{(N)}(0) = -\frac{1}{4}\epsilon$], to the random-walk result, $\bar{\mu}_N(0) = 0$ [i.e., $\bar{E}^{(N)}(\frac{1}{2}) = 0$].

At fixed N —however large—the width vanishes in both limits $\delta \rightarrow 1$ ($A \rightarrow 0$) and $\delta \rightarrow -1$ ($D \rightarrow 0$), and $\bar{\mu}_N(\delta)$ lands on either the purely diabatic or adiabatic path. Evaluation of Eqs. (27) and (31) to lowest order in $2AN$ yields, for the diabatic limit,

$$\bar{\mu}_N(\delta) \pm \Delta\mu_N(\delta) \xrightarrow{A \rightarrow 0} N - AN(N+1) \pm \sqrt{\frac{2}{3}AN(N+1)(2N+1)}, \quad \text{fixed } N \quad (35)$$

in analogy to Eq. (34). [Note that $\mu = N$ corresponds to $E = E_0(t^{(N)})$.] At $\delta < 0$, one must distinguish between even and odd N ; to lowest order in $2DN$, the adiabatic limit yields

$$\bar{\mu}_N(\delta) \pm \Delta\mu_N(\delta) \xrightarrow{D \rightarrow 0} \begin{cases} 0 - DN \pm \sqrt{2DN}, & \text{fixed } N \text{ even} \\ -1 + D(N+1) \pm \sqrt{2D(N+1)}, & \text{fixed } N \text{ odd} \end{cases} \quad (36)$$

The average position for successive odd-even generations is indeed $\bar{\mu}_N(-1) = -\frac{1}{2}$.

In all cases, therefore, *the concentration of population $P_{mm'}^{(N)}(D)$ eventuates somewhere near the center of the interaction region* and broadens slowly with $\Gamma^{(N)}(D) \propto \sqrt{N}$. The fact that paths tend, on the average, to steer towards the center rather than the edges of the grid contributes to the stabilization of the average energy at large N . *Only in the extreme diabatic limit $A \ll 1/2N$ is there any significant departure from a quasisymmetric distribution centered at some energy closer to $E=0$ than the distribution's width.* All adiabatic cases $-1 \leq \delta \leq 0$ ($0 \leq D \leq \frac{1}{2}$) are essentially narrow versions of a random walk centered just below $E=0$.

V. GENERATING FUNCTION

The statistically derived probability expressions (16)–(20) of Sec. III are exact for the two-manifold,

parallel-level model. However, an alternative treatment based on recursion relations leads to more compact versions of these expressions in terms of 2×2 matrices. The generating function derived here for $P_{mm'}^{(N)}(D)$ is computationally convenient and may prove useful in studies involving interference between paths.

The populations of any pair of up- and down-going level segments $m^{(N)}$ and $m'^{(N)}$ mix in the vicinity of their LZ anticrossing $[m, m']$ and emerge onto $m^{(N+1)}$ and $m'^{(N+1)}$ with probabilities:

$$P_{m, m'+1, \uparrow}^{(N+1)}(D) = DP_{mm', \uparrow}^{(N)}(D) + AP_{mm', \downarrow}^{(N)}(D), \quad (37a)$$

$$P_{m+1, m', \downarrow}^{(N+1)}(D) = AP_{mm', \uparrow}^{(N)}(D) + DP_{mm', \downarrow}^{(N)}(D). \quad (37b)$$

the value of $\mu = m' - m$ increases by 1 in Eq. (37a) and decreases by 1 in Eq. (37b). One can keep track of different μ values by multiplying each probability by $x^{m'-m}$, where x is an expansion parameter. The distributions of probabilities for approaching any intersection at $t = t^{(N)}$ on one manifold or the other is then provided by a coefficient in either polynomial

$$\mathcal{P}_{\uparrow}^{(N)}(D; x) \equiv \sum_{m=0}^N P_{mm', \uparrow}^{(N)}(D) x^{m'-m} \delta_{m', N-m}, \quad (38a)$$

or

$$\mathcal{P}_{\downarrow}^{(N)}(D; x) \equiv \sum_{m=0}^N P_{mm', \downarrow}^{(N)}(D) x^{m'-m} \delta_{m', N-m}. \quad (38b)$$

The recursion relations (37) can then be cast into the matrix form [20]

$$\begin{bmatrix} \mathcal{P}_{\uparrow}^{(N+1)}(D; x) \\ \mathcal{P}_{\downarrow}^{(N+1)}(D; x) \end{bmatrix} = \begin{bmatrix} Dx & Ax \\ Ax^{-1} & Dx^{-1} \end{bmatrix} \begin{bmatrix} \mathcal{P}_{\uparrow}^{(N)}(D; x) \\ \mathcal{P}_{\downarrow}^{(N)}(D; x) \end{bmatrix}. \quad (39)$$

If we define $\mathcal{P}^{(N)}(D; x) \equiv \mathcal{P}_{\uparrow}^{(N)}(D; x) + \mathcal{P}_{\downarrow}^{(N)}(D; x)$, seed Eq. (39) with the initial values $\mathcal{P}_{\uparrow}^{(0)}(D; x) = 1$ and $\mathcal{P}_{\downarrow}^{(0)}(D; x) = 0$, and iterate, we obtain a polynomial whose coefficients represent the total probability distribution at generation N :

$$\begin{aligned} \mathcal{P}^{(N)}(D; x) &\equiv \sum_{m=0}^N P_{mm'}^{(N)}(D) x^{m'-m} \delta_{m', N-m} \\ &= (1 \ 1) \left[\begin{bmatrix} x & 0 \\ 0 & x^{-1} \end{bmatrix} \begin{bmatrix} D & A \\ A & D \end{bmatrix} \right]^N \begin{bmatrix} 1 \\ 0 \end{bmatrix}. \end{aligned} \quad (40)$$

$\mathcal{P}_{\uparrow}^{(N)}(D; x)$ and $\mathcal{P}_{\downarrow}^{(N)}(D; x)$ can be obtained by replacing the row vector in Eq. (40) with $(1 \ 0)$ and $(0 \ 1)$, respectively. Note that $\mathcal{P}^{(N)}(D; 1) = 1$ for any D and N , a statement of normalization at all times.

To calculate the average $\bar{\mu}_N(\delta)$ [Eqs. (26)–(27)] with the generating function (40), one must apply $\partial/\partial x$ to $\mathcal{P}^{(N)}(D; x)$ and evaluate at $x = 1$. It is convenient first to substitute the diagonalized form of the matrix $\begin{pmatrix} D & A \\ A & D \end{pmatrix}$ into Eq. (40):

$$\mathcal{P}^{(N)}(D; x) = (1 \ 0) \left[\frac{1}{2} \begin{bmatrix} 1 & 1 \\ 1 & -1 \end{bmatrix} \begin{bmatrix} x & 0 \\ 0 & x^{-1} \end{bmatrix} \begin{bmatrix} 1 & 1 \\ 1 & -1 \end{bmatrix} \begin{bmatrix} 1 & 0 \\ 0 & \delta \end{bmatrix} \right]^N \begin{bmatrix} 1 \\ 1 \end{bmatrix}. \quad (41)$$

Application of $\partial/\partial x$ and the chain rule to the product of N matrices in Eq. (41), each including a factor

$$\mathbf{X} = \begin{pmatrix} x & 0 \\ 0 & x^{-1} \end{pmatrix},$$

yields

$$\begin{aligned} \bar{\mu}_N(\delta) &= \left. \frac{\partial \mathcal{P}^{(N)}(D; \mathbf{x})}{\partial x} \right|_{x=1} \\ &= \sum_{j=0}^{N-1} (1 \ 0) \begin{pmatrix} 1 & 0 \\ 0 & \delta \end{pmatrix}^{N-1-j} \left[\begin{pmatrix} 0 & 1 \\ 1 & 0 \end{pmatrix} \begin{pmatrix} 1 & 0 \\ 0 & \delta \end{pmatrix} \right] \begin{pmatrix} 1 & 0 \\ 0 & \delta \end{pmatrix}^j \begin{pmatrix} 1 \\ 1 \end{pmatrix} \\ &= (1 \ 0) \begin{pmatrix} 0 & \delta \\ 1 & 0 \end{pmatrix} \begin{pmatrix} 1 & 0 \\ 0 & \sum_{j=0}^{N-1} \delta^j \end{pmatrix} \begin{pmatrix} 1 \\ 1 \end{pmatrix} = \sum_{j=1}^N \delta^j, \end{aligned} \quad (42)$$

the same result as Eq. (27).

A calculation of the standard deviation $\Delta\mu_N(\delta)$ requires here only the verification of the form (30) for $\bar{\mu}_N^2(\delta)$. The second moment of $(m' - m)$ in Eq. (41) is given by

$$\begin{aligned} \bar{\mu}_N^2(\delta) &= \left[\frac{\partial^2 \mathcal{P}^{(N)}(D; \mathbf{x})}{\partial x^2} + \frac{\partial \mathcal{P}^{(N)}(D; \mathbf{x})}{\partial x} \right]_{x=1} \\ &= 2 \sum_{j=0}^{N-2} \sum_{k=0}^{N-2-j} (1 \ 0) \begin{pmatrix} 1 & 0 \\ 0 & \delta \end{pmatrix}^{N-2-j-k} \begin{pmatrix} 0 & \delta \\ 1 & 0 \end{pmatrix} \begin{pmatrix} 1 & 0 \\ 0 & \delta \end{pmatrix}^k \begin{pmatrix} 0 & \delta \\ 1 & 0 \end{pmatrix} \begin{pmatrix} 1 & 0 \\ 0 & \delta \end{pmatrix}^j \begin{pmatrix} 1 \\ 1 \end{pmatrix} \\ &\quad + \sum_{j=0}^{N-1} (1 \ 0) \begin{pmatrix} 1 & 0 \\ 0 & \delta \end{pmatrix}^{N-1-j} \left[\begin{pmatrix} 1 & -1 \\ -1 & 1 \end{pmatrix} + \begin{pmatrix} 0 & 1 \\ 1 & 0 \end{pmatrix} \right] \begin{pmatrix} 1 & 0 \\ 0 & \delta \end{pmatrix}^{j+1} \begin{pmatrix} 1 \\ 1 \end{pmatrix}. \end{aligned} \quad (43)$$

The two bracketed terms in the single sum come from second and first derivatives of the matrix \mathbf{X} ; this whole series reduces to just N . The double sum in Eq. (43) stems from the cross terms in $\partial^2 \mathcal{P}^{(N)}/\partial x^2$. Evaluation and reindexing of the double sum leads directly to the results (30) for $\bar{\mu}_N^2(\delta)$ and the half-width (31).

The statistical results of Sec. III, Eqs. (16)–(21), also follow from suitable manipulations of Eq. (40) or Eq. (41). The binomial coefficients in Eq. (19) arise from derivatives $\partial^\mu/\partial x^\mu$ applied to the N factors \mathbf{X} , evaluated at $x=0$.

VI. DISCUSSION

The present model of incoherent evolution on a Landau-Zener grid of two interacting manifolds yields analytical results for the redistribution of population throughout the levels of both manifolds when only one state is initially populated. The assumption of parallel energy levels at high n and the neglect of interference effects are not critical to general features of the distribution, such as the concentration of population near the center of the interaction region and the ramp dependence of the distribution's width after long times. Since SFI experiments can resolve only bands of states within each manifold anyway [5], it is important to be able to characterize at least the grossest features of the mixing before attending to substructures that may appear in the ionization signals.

The simple model considered here should, however, be modified in several ways to better represent an atom subjected to a field $F(t)$. True manifolds of Rydberg levels are not parallel, nor is the LZ parameter $\gamma_{n'_1 n_1}$ given just by γ [Eqs. (7) and (8)]: The couplings $v_{n'_1 n_1, 0, nn_1, 0}$ as well as the slope differences $|p - p'|$ vary from one anticrossing to another. (Note, however, that as long as one invokes the LZ approximation, the fanning out of each manifold's levels would not alter the topology of the network.) For a pure- s core, although

$$v_{n'_1 n_1, 0, nn_1, 0} = -\mu_0 (n' n)^{-2}$$

for all pairs of levels, the fact that the slopes of midmanifold levels are smaller than for edge states implies that adiabatic transitions for $n_2 = m > 0$ or $n'_1 = m' > 0$ are more probable than in the present model. In that case, nonedge slopes $dE_{nn_1 n_2 0}/dt$ and $dE_{n'_1 n'_1 n'_2 0}/dt$ obtained from Eq. (4) have a difference

$$|p - p'| = 3\dot{F} n^2 (1 - N/n)$$

common to all intersections of generation N (assuming $n \gg 1$ and $N = n_2 + n'_1 < n$). Then the LZ exponent $\gamma_{n'_1 n_1}$ in Eq. (7) would be larger than the value $|\mu_0|^2/3\dot{F} n^{10}$ [Eq. (8)] by the factor $(1 - N/n)^{-1}$, reducing the diabatic-transition probability for that generation from D to $D_N = D^{n/(n-N)}$. The analytical results of Secs. III, IV,

and V could then be modified using the various values $\{\delta_N = 2D_N - 1\}$, e.g., the average level position in Eq. (27) would become

$$\bar{\mu}_N = \delta_0 + \delta_0 \delta_1 + \delta_0 \delta_1 \delta_2 + \cdots + (\delta_0 \cdots \delta_{N-1}), \quad (44)$$

yielding a “more adiabatic” result than that for all δ_N 's equal to δ_0 . Furthermore, the spreading of level distributions would not go on as $\sim \sqrt{N}$ but instead “freeze out” at early times $t^{(N)}$, for a given ramp rate, because the diabatic transitions that give rise to diffusion in energy would be less likely to occur. The inclusion of non-negligible quantum defects for $l \geq 1$ would further enhance adiabatic transitions involving midmanifold states when $|m_l| \approx l$ while enhancing diabatic transitions involving edge states [15] (but have the opposite effect when $l > 1$ and $|m_l| \ll l$) due to the behavior of the squared coefficients [12] in Eq. (2).

Additional modifications would, however, change the model qualitatively. Interference between the different paths leading to each $[m, m']$ has been found to produce resonance series in $P_{mm'}^{(N)}(D)$ rather than a single-humped distribution [8]. Completely abandoning the LZ approximation and allowing simultaneous multilevel interference among two entire manifolds [17], then including a third manifold, etc., would constitute the most liberal version of the model—one closer to SFI. While more general analytical results are possible under certain assumptions [21], their interpretation may, however, be far from transparent.

In an SFI experiment, a band of levels may be initially excited rather than just one. To represent this most simply within the present model of parallel levels and incoherent evolution, one might, for example, equally populate all levels $m^{(m)}$ ($m = 0, 1, \dots$) of one manifold. The probability at intersection $[m, m']$ ($m + m' = N$) would then be expressible in terms of the result (19) for one ini-

tial state:

$$(N+1)^{-1} \sum_{j=0}^m P_{m-j, m'}^{(N-j)}(D). \quad (45)$$

In the diabatic limit all levels of generation N become equally populated, whereas in the adiabatic limit the levels in the lower half of the grid become equally populated (i.e., \uparrow level segments $m^{(N)}$ with $m \geq \frac{1}{2}N$, \downarrow segments $m'^{(N)}$ with $m' < \frac{1}{2}N$) while those in the upper half remain unpopulated. For generic intermediate cases, one finds that the population distribution rises from relatively small values for intersections at $E > 0$ (i.e., with $m < m'$) to a plateau for levels at lower energies (i.e., $m > m'$). The step at midgrid ($m \approx m'$) is steeper the smaller is D . The plateau at time $t^{(N)}$ attains its maximum value, $(2 - D^N)/(N + 1)$, at the lowest intersection, $[N, 0']$.

A physical system that realizes the redistribution of population for the LZ grid is an analogous grid of partially silvered mirrors, one per $[m, m']$, with flat surfaces oriented parallel to the time axis of Fig. 2. A light beam of intensity I_0 impinging on the first mirror in the same way that level 0 approaches $[0, 0']$ would branch and arrive at subsequent mirrors with intensity $P_{mm'}^{(N)}(D)I_0$, where D is now each mirror's transmission probability. Interference could be avoided or exploited by preventing or allowing mixing of the beams at each mirror.

ACKNOWLEDGMENTS

The authors would like to thank Dr. M. J. Cavagnero and Dr. K. B. MacAdam for many helpful discussions. This work is supported by the U.S. Department of Energy, Division of Chemical Sciences, Office of Basic Energy Sciences, Offices of Energy Research, under Grant No. DE-FG05-92ER14267.

- [1] *Atoms in Strong Fields*, edited by C. A. Nicolaides, C. W. Clark, and M. H. Nayfeh (Plenum, New York, 1990).
- [2] M. L. Zimmerman, M. G. Littman, M. M. Kash, and D. Kleppner, *Phys. Rev. A* **20**, 2251 (1979).
- [3] D. A. Harmin, *Phys. Rev. A* **30**, 2413 (1984).
- [4] H. Nakamura, *Int. Rev. Phys. Chem.* **10**, 123 (1991).
- [5] *Rydberg States of Atoms and Molecules*, edited by R. F. Stebbings and F. B. Dunning (Cambridge University Press, New York, 1983), Chaps. 3 and 9; K. B. MacAdam, L. G. Gray, and R. G. Rolfs, *Phys. Rev. A* **42**, 5269 (1990).
- [6] L. Landau, *Phys. Z. Sowjun* **2**, 46 (1932); C. Zener, *Proc. R. Soc. London, Ser. A* **137**, 696 (1932); E. C. G. Stueckelberg, *Helv. Phys. Acta* **5**, 369 (1932).
- [7] L. D. Landau and E. M. Lifshitz, *Quantum Mechanics of One- and Two-Electron Atoms (Non-Relativistic Theory)* (Pergamon, Oxford, 1976); see, especially, Sec. 90.
- [8] D. A. Harmin, *Bull. Am. Phys. Soc.* **38**, 1096 (1993); D. A. Harmin (unpublished).
- [9] We assume, following Ref. [3], that all quantum defects are expressed modulo 1 and lie in the range $-\frac{1}{2} < \mu_l \pmod{1} \leq \frac{1}{2}$.

- [10] See, e.g., H. A. Bethe and E. E. Salpeter, *Quantum Mechanics of One- and Two-Electron Atoms* (Springer, Berlin, 1957). One of the parabolic quantum numbers describing the state $|nn_1n_2m_l\rangle$ is actually redundant since $n = n_1 + n_2 + |m_l| + 1$.
- [11] D. A. Harmin, *Phys. Rev. A* **44**, 433 (1991).
- [12] The notation here differs from that in Ref. [11] by the relabeling of the state index from a subscript “ p ” (which equals $n_1 - n_2$) to “ n_1 ” to avoid confusion with the particular slopes defined here in Eq. (6). Table III of Ref. [11] gives explicit transformation coefficients for $l = 0 - 3$; note the normalization $\sum_{n_1=0}^{n-1} \mu_{n_1 l}^{(n_0)} \mu_{n_1 l'}^{(n_0)} = n \delta_{ll'}$. See also D. A. Harmin, in Ref. [1], p. 61, Sec. III E.
- [13] By way of comparison, multiphoton excitation and ionization of hydrogen ($n \sim 28$) can be accomplished via microwave fields $F(t) = F_0 \cos(\omega t)$ at frequencies $\omega/2\pi \sim 10$ GHz and amplitudes $F_0 \sim 100$ V/cm. The peak derivative $\omega F_0 \sim 5 \times 10^{12}$ (V/cm)/s is much larger than typical linear rates $\dot{F} \lesssim 10^9$ (V/cm)/s used for SFI, which would not be able to drive intermanifold transitions efficiently. For microwave ionization, see D. R. Mariani, W. van de Water, P. M. Koch, and T. Bergeman, *Phys. Rev. Lett.* **50**, 1261

(1983); W. van de Water *et al.*, Phys. Rev. A **42**, 572 (1990). For SFI, see Ref. [5].

[14] I. V. Komarov, T. P. Grozdanov, and R. K. Janev, J. Phys. B **13**, L573 (1980); W. van de Water, D. R. Mariani, and P. M. Koch, Phys. Rev. A **30**, 2399 (1984).

[15] These remarks apply to $m_l=0$; the gaps are smaller for $m_l \neq 0$. For $m_l \geq 0$ and a single quantum defect for $l=m_l$, the edge states ($n_1 \rightarrow n$ or 0) have $|u_{n_1 l}^{(nm_l)} \delta_{lm_l}|^2 \sim O(n^{-m_l})$ and gap size $|2v| \sim 2|\mu|/n^{4+m_l}$, i.e., smaller than the Stark splitting by a further factor n^{-m_l} .

[16] M. R. Spalburg, J. Los, and A. Z. Devdariani, Chem. Phys. **103**, 253 (1986); K. Mullen, E. Ben-Jacob, Y. Gefen, and Z. Schuss, Phys. Rev. Lett. **62**, 2543 (1989).

[17] Several key results in Secs. III and IV, particularly Eqs. (16), (17), (27), and (31), were also derived in Phillip N. Price, Ph.D. dissertation, University of Kentucky, 1992.

[18] Equations (16) and (17) can also be expressed as hypergeometric functions (for $m \neq 0$):

$$P_{mm'}^{(N)\uparrow}(D) = D^N [F(-m, -m'; 1; A^2/D^2) - F(1-m, -m'; 1; A^2/D^2)],$$

$$P_{mm'}^{(N)\downarrow}(D) = AD^{N-1} F(1-m, -m'; 1; A^2/D^2).$$

[19] Yu. N. Demkov, Dokl. Acad. Nauk SSSR **166**, 1076 (1966) [Sov. Phys.—Dokl. **11**, 138 (1966)]; Yu. N. Demkov and V. I. Osherov, Zh. Eksp. Teor. Fiz. **53**, 1589 (1967) [Sov. Phys.—JETP **26**, 916 (1968)]. See also Y. Kayanuma and S. Fukuchi, J. Phys. B **18**, 4089 (1985).

[20] Equations (37a)–(37b) can be combined to yield recursion relations for either up- or down-going levels alone:

$$P_{m+1, m'+1, \uparrow}^{(N+2)}(D) = DP_{m+1, m', \uparrow}^{(N+1)}(D) + DP_{m, m'+1, \uparrow}^{(N+1)}(D) - (D-A)P_{mm'}^{(N)\uparrow}(D),$$

plus an identical relation for $P_{mm'}^{(N)\downarrow}(D)$. Replacing differences by derivatives in m and m' then leads to the differential equation $\partial P/\partial m + \partial P/\partial m' + (1/A)\partial^2 P/\partial m \partial m' = 0$, where P stands for either $P_{mm'}^{(N)\uparrow}(D)$ or $P_{mm'}^{(N)\downarrow}(D)$. However, superposing solutions of this equation to obtain an analytical form for $P_{mm'}^{(N)}(D)$ is less practical than direct use of Eq. (19) or Eq. (40).

[21] See, e.g., R. K. Janev and P. S. Krstić, J. Phys. B **19**, 3695 (1986).